Offprinted from the *Journal of The Chemical Society, Faraday Transactions II*, 1975, vol. 71.

Effect of $\Delta J = 4$ Transitions on the Far Infra-red Normalised Lineshapes of O_2, CO_2 and $(CN)_2$ Gases

BY MYRON EVANS*†

Edward Davies Chemical Laboratories,
The University College of Wales, Aberystwyth SY23 1NE

Received 9th October, 1974

Fourier transforms of the far infra-red pressure induced absorption bands in O_2, CO_2, and $(CN)_2$ gases are compared with theoretical expressions derived from $\Delta J = 2$ and $\Delta J = 4$ (quadrupole and hexadecapole induced) line intensities. Satisfactory matching of theoretical and experimental normalised lineshapes displayed through the corresponding time domain functions, is obtained for O_2 and CO_2, but not for $(CN)_2$. Reasons for these findings are discussed.

This work aims to explain the discrepancies found between theoretical [1-3] and experimental [4-6] normalised bandshapes for the far infra-red (3-450 cm^{-1}) pressure-induced absorptions in oxygen, carbon dioxide, and cyanogen gases. Here, the hexadecapole-induced dipole absorptions ($J \rightarrow J+4$, where J is the rotational quantum number) are taken into consideration in addition to the usual quadrupole induced ones ($J \rightarrow J+2$).

Linear, non-dipolar molecules like O_2, CO_2 and $(CN)_2$ have no net charge, no dipole moment, and no octupole moment by symmetry. They do have quadrupole (Q) and hexadecapole (Φ) moments, and Frost's theory [7] allows these to be taken into account. The spectral consequences of this modification are summarised in eqn (1):

$$A_{\text{exp}} = \int_0^\infty \alpha(\bar{\nu})\,\mathrm{d}\bar{\nu} = \left(\sum_J A^Q_{J\rightarrow J+2}Q^2 + \sum_J A^\Phi_{J\rightarrow J+4}\Phi^2\right)N^2. \tag{1}$$

Here the experimental integrated absorption (A_{exp}) is represented on the r.h.s. of eqn (2) by the terms:

$$A^Q_{J\rightarrow J+2} = \frac{4\pi^3}{3hcZ}\int_0^\infty 4\pi R^{-6}\exp(-U_{AA}(R)/kT)\,\mathrm{d}R[1-\exp(-hc\bar{\nu}_2(J)/kT)]\times \exp(-E_Jhc/kT)\bar{\nu}_2(J)\left[\frac{9\alpha_0^2(J+1)(J+2)}{(2J+3)}+\frac{18}{5}\delta^2\left(\frac{(J+1)(J+2)}{(2J+3)}\right)^2\right] \tag{2}$$

$$A^\Phi_{J\rightarrow J+4} = \frac{4\pi^3}{3hcZ}\int_0^\infty 4\pi R^{-10}\exp(-U_{AA}(R)/kT)\,\mathrm{d}R[1-\exp(-hc\bar{\nu}_4(J)/kT)]+ \exp(-E_Jhc/kT)\bar{\nu}_4(J)\left[\frac{175(J+1)(J+2)(J+3)(J+4)\alpha_0^2}{2(2J+3)(2J+5)(2J+7)}+ \frac{875}{12}\delta^2\left(\frac{(J+1)(J+2)}{(2J+3)}\right)^2\frac{(J+3)(J+4)}{(2J+5)(2J+7)}\right]. \tag{3}$$

† present address: Physical Chemistry Laboratory, South Parks Road, Oxford OX1 3QZ.

N is the molecular number density (molecules cm^{-3}), α_0 the mean molecular polarisability, δ the anisotropy of the polarisability, and Z the rotational partition function. E_J represents the rotational energy levels for rigid, linear molecules, given by:

$$E_J = BJ(J+1).$$

In addition:

$$\bar{\nu}_2(J) = 2B(2J+3)$$

where $\Delta J = 2$, i.e., quadrupole induced dipolar transitions; and:

$$\bar{\nu}_4(J) = 4B(2J+5)$$

where $\Delta J = 4$, i.e., hexadecapole induced dipolar transitions.

The experimental bands [4-6] [$\alpha(\nu)$ contours] observed in non-dipolar compressed gases in the far infra-red are broad [$(\Delta\bar{\nu})_{1/2} \approx 80\ cm^{-1}$] and continuous, whereas the discrete eqn (1) yields two sets of line spectra [$\delta(\nu)$ functions] corresponding to $\Delta J = 2$ and $\Delta J = 4$ transitions. Comparison between theory and experiment is facilitated if eqn (1) can be manipulated into a continuous form, conveniently with time as the variable. This can be done [1, 8, 9] by Fourier transforming the respective experimental and theoretical normalised spectral densities [$I(\nu)$] from the frequency to the time domain.

The usual expression [10] for a rotational absorption band shape, in terms of transitions between quantum states is:

$$I(\omega) = \frac{3\hbar c\sigma(\omega)}{4\pi^2\omega[1-\exp(-\hbar\omega/kT)]} \tag{4}$$

where $\omega = 2\pi\bar{\nu}c$, and σ is the absorption cross section per molecule. The Fourier transform:

$$F(t) = \int_{-\infty}^{\infty} \omega^2 I(\omega)\exp(i\omega t)\,d\omega \tag{5}$$

being recommended by Gordon [10] and used here to weight the intensity towards the higher frequencies ($10 \lesssim \bar{\nu} \lesssim 450\ cm^{-1}$) where accurate data are available. Here, $\sigma(\omega) = \alpha(\omega)/N$.

Fourier transforms, via eqn (5), are made on:

(i) experimental [4-6] results on the far infra-red pressure induced absorption bands of O_2, CO_2, and $(CN)_2$;

(ii) $\alpha(\bar{\nu})$ from eqn (1).

The resulting curves, normalised to unity at $t = 0$, are compared in fig. 1-3.

The theoretical functions of time, $F_{th}(t)$ are obtained by substituting eqn (1) into (5), it being convenient [8] to use the continuous expression for the contours passing through the points of $I(\bar{\nu})$ obtained from (1) by eliminating J in $A^{Q}_{J\to J+2}$ and $A^{\Phi}_{J\to J+4}$ on the bases $\bar{\nu}_2(J) = 2B(2J+3)$ and $\bar{\nu}_4(J) = 4B(2J+5)$ respectively. One then has the theoretical spectral intensity $I_{th}(\bar{\nu})$ as:

$$\begin{aligned} I_{th}(\bar{\nu}) \propto {} & \left(\frac{\bar{\nu}}{2B}-\frac{2B}{\bar{\nu}}\right)Q^2 \exp\left[-\frac{hcB}{4kT}\left(\frac{\bar{\nu}}{2B}-3\right)\left(\frac{\bar{\nu}}{2B}-1\right)\right]A_8\left[12\alpha_0^2+\frac{24}{5}\left(\frac{\bar{\nu}}{2B}-\frac{2B}{\bar{\nu}}\right)\delta^2\right]+ \\ & \frac{(\bar{\nu}+4B)(\bar{\nu}+12B)}{\bar{\nu}(\bar{\nu}+8B)}\Phi^2 \exp\left[-\frac{hcB}{4kT}\left(\frac{\bar{\nu}}{4B}-5\right)\left(\frac{\bar{\nu}}{4B}-3\right)\right]\times \\ & A_{12}\left[\tfrac{175}{96}\alpha_0^2\left(\frac{(\bar{\nu}-12B)(\bar{\nu}-4B)}{B(\bar{\nu}-8B)}\right)+\tfrac{875}{36}\delta^2\left(\frac{\bar{\nu}}{2B}-\frac{2B}{\bar{\nu}}\right)^2\right] \end{aligned} \tag{6}$$

where

$$A_n = \frac{\pi^3 N^2}{hcZ} \int_0^\infty 4\pi^2 R^{-n} \exp(-U_{AA}(R)/kT) R^2 \, dR.$$

Thus from (5),

$$F_{th}(t) = \int_{-\infty}^{\infty} I_{th}(\bar{\nu})\bar{\nu}^2 \exp(2\pi i\bar{\nu}ct)\, d\bar{\nu} \Big/ \int_{-\infty}^{\infty} I_{th}(\bar{\nu})\bar{\nu}^2 \, d\bar{\nu}, \tag{7}$$

the corresponding experimental function being:

$$F_{exp}(t) = \int_{-\infty}^{\infty} \frac{\bar{\nu}\alpha(\bar{\nu}) \exp(2\pi i\bar{\nu}ct)\, d\bar{\nu}}{(1-\exp(-hc\bar{\nu}/kT))} \Big/ F_{exp}(0). \tag{8}$$

Sources of absorption which are neglected in this work because their quantitative treatment is difficult are listed as follows.

(i) Absorption due to translational effects in a bimolecular collision ($\Delta J_1 = \Delta J_2 = 0$). Ho *et al.*[5] have estimated an important contribution from this source in CO_2.

(ii) Absorption due to collisions involving more than two molecules, leading to underdamping of the time domain cosine curves obtained by Fourier transformation of the theoretical curves.

(iii) The theoretical line spectra are derived assuming that the intermolecular potential energy [$U_{AA}(R)$] is a function of the intermolecular separation (R) only, the form being approximated by the Lennard-Jones function. For anisotropic molecules such as cyanogen, the quadrupole–quadrupole interaction energy (U_{QQ}) is important and angle-dependent. Therefore the eigenstate of an interacting molecular pair cannot be accurately taken as the product of those of the isolated molecules as the simplified theory [2, 3] demands.

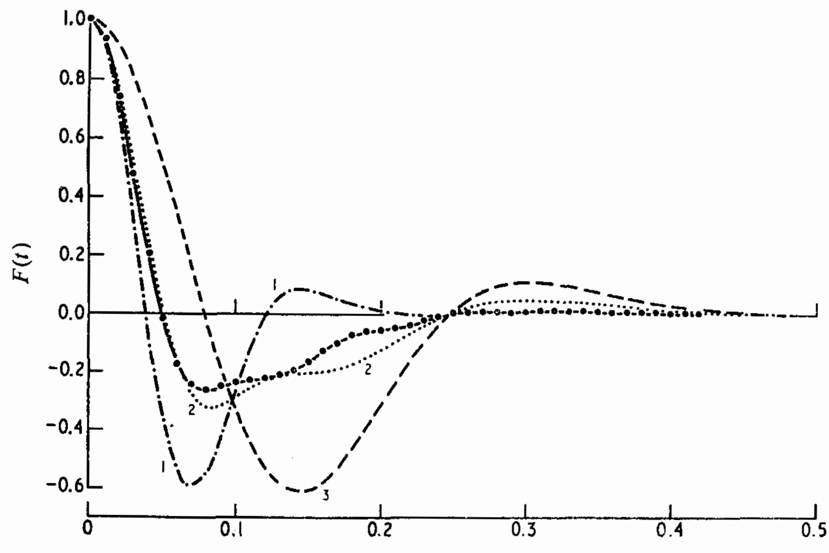

FIG. 1.—Fourier transforms for O_2 gas at 300 K, 35-75 amagat.[4] ●-●-● $F_{exp}(t)$ as derived from two separate algorithms. ---- (1) $F_{th}(t)$ calculated with $|Q| = 0.30 \times 10^{-26}$ e.s.u., $|\Phi| = 1.1 \times 10^{-42}$ e.s.u. (2) $F_{th}(t)$ with $|Q| = 0.36 \times 10^{-26}$ e.s.u. $|\Phi| = 0.4 \times 10^{-42}$ e.s.u. (3) $F_{th}(t)$ with $|Q| = 0.38 \times 10^{-26}$ e.s.u., $|\Phi| = 0$.

COMPUTATIONAL DETAILS

$F_{exp}(t)$ was computed with two quite different algorithms. The first is a Simpson's rule integration of the cosine part of (8), giving the solid curves in fig. 1-3.

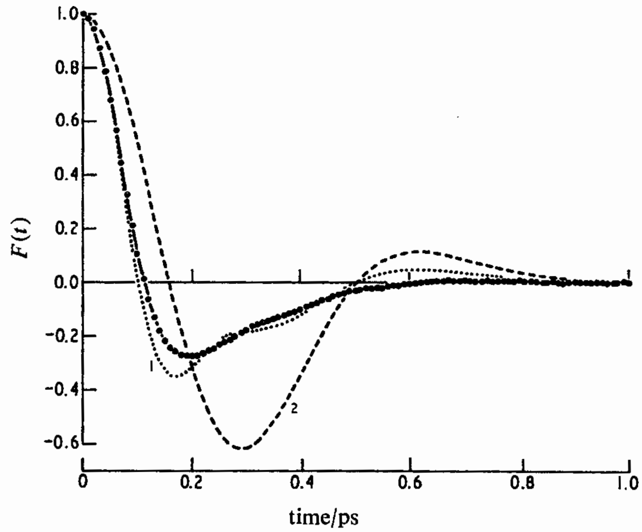

FIG. 2.—Fourier transforms for CO_2 gas at 273 K, 85 amagat.[5] ●-●-● $F_{exp}(t)$ as derived from two separate algorithms. ---- (1) $F_{th}(t)$ with $|Q| = 5.0 \times 10^{-26}$ e.s.u., $|\Phi| = 6.1 \times 10^{-42}$ e.s.u. (2) $F_{th}(t)$ with $|Q| = 5.2 \times 10^{-26}$ e.s.u., $|\Phi| = 0$.

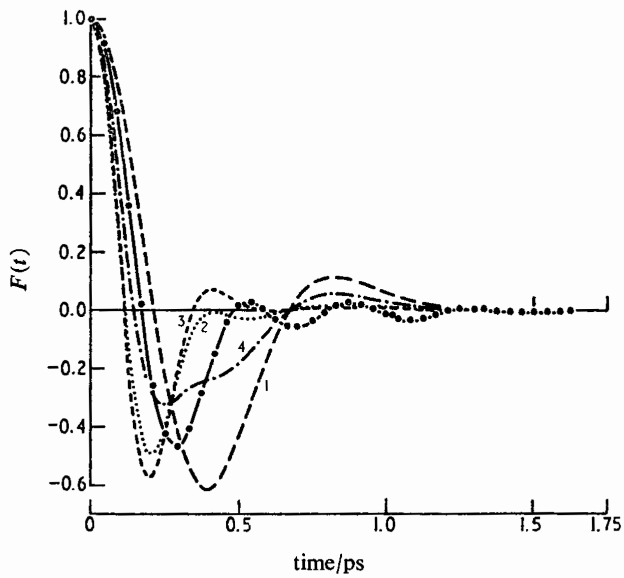

FIG. 3.—Fourier transforms for $(CN)_2$ gas at 383 K, 33.5 bar.[6] ●-●-● $F_{exp}(t)$ as derived from two separate algorithms. ---- (1) $F_{th}(t)$ with $|Q| = 15.5 \times 10^{-26}$ e.s.u., $|\Phi| = 0$. (2) $F_{th}(t)$ with $|Q| = 12.0 \times 10^{-26}$ e.s.u., $|\Phi| = 44 \times 10^{-42}$ e.s.u. (3) $F_{th}(t)$ with $|Q| = 9.0 \times 10^{-26}$ e.s.u., $|\Phi| = 56 \times 10^{-42}$ e.s.u. (4) $F_{th}(t)$ with $|Q| = 14.5 \times 10^{-26}$ e.s.u., $|\Phi| = 24 \times 10^{-42}$ e.s.u.

The second is a Fast Fourier Transform (F.F.T.) as implemented in algol by Singleton,[11, 12] and used previously by Baise [8]; the experimental data in both cases being sampled at discrete intervals $\Delta\bar{\nu}$ small enough to prevent aliasing, or overlapping of the computed curves. The second algorithm gives the points plotted in fig. 1-3. $F_{th}(t)$ was evaluated with the F.F.T. to give the dashed curves. The integrals A_n were worked out with the well-known tables of Buckingham and Pople,[13] assuming therefore that $U_{AA}(R)$ is radial. The values of the molecular constants used are tabulated below.

TABLE 1.—MOLECULAR CONSTANTS USED IN COMPUTING $F_{th}(t)$

gas	temp./K	pressure	B/cm^{-1}	(ε/k)K	$\sigma/\text{Å}$	$10^{24}\alpha_0$ /cm³	$10^{24}\delta$ /cm³	$10^{26}\lvert Q\rvert$ /e.s.u.	$10^{42}\lvert\Phi\rvert$ /e.s.u.
O_2	300	35-75 amagat	1.45	118	3.46	1.60	1.14	0.36	0.4
CO_2	273	85 amagat	0.393	219	3.82	2.196	1.75[14]	5.0	6.1
(CN_2)	383	33.5 bar	0.1571	339	4.38	4.38	4.12	12	44

$|Q|$ and $|\Phi|$ are the values which give the best fit to $F_{exp}(t)$. Q^2 and Φ^2 are not independent variables, being related via eqn (1) to the experimental integrated intensity A_{exp}. The absolute values were fixed from previous [4-6] estimations where the Φ^2 dependence was neglected, the whole of A_{exp} being attributed in these to quadrupole induced dipole absorption alone, giving previous values of $|Q| = 0.38\times10^{-26}$ e.s.u. for O_2, 5.2×10^{-26} e.s.u. for CO_2 and 15.5×10^{-26} e.s.u. for $(CN)_2$.

RESULTS

OXYGEN

$F_{th}(t)$ seems to be extraordinarily sensitive to small changes in $|Q|$ and $|\Phi|$. This is illustrated in fig. 1, where a previous frequency domain curve fitting, using values of $|Q| = 0.30\times10^{-26}$ e.s.u. $|\Phi| = 1.1\times10^{-42}$ e.s.u. yields a corresponding $F_{th}(t)$ which is quite severely underdamped compared with $F_{exp}(t)$. However, using values of $|Q|$ and $|\Phi|$ given in table 1 results in a much better match, $F_{th}(t)$ now showing very short time " oscillations ", although they are slightly displaced along the time axis from those of $F_{exp}(t)$. Possible causes of the remaining lineshape discrepancy are as follows:

(i) Translational absorption, which is more likely [4, 5] to affect the long-time tail of $F(t)$.

(ii) Triple collisions, which would need a N^3 term in (1).

(iii) Because of the wide separation (only even J allowed from nuclear spin statistics) of each $J\rightarrow J+2$ and $J\rightarrow J+4$ line, the extraction of a continuous time domain function F_{th} by effectively transforming the sum of the profiles of the $\delta(\nu)$ functions may be affected by neglect of the actual broadening of each line observed in practice. After all, the experimental absorption is a broad curve and not an assembly of lines. Curve 3 in fig. 1, where the Φ^2 term is neglected, corresponds to the profile of the bar spectrum of $\Delta J = 2$ lines given by Bosomworth and Gush in their paper [4] on compressed O_2.

CARBON DIOXIDE

The best agreement between $F_{exp}(t)$ and $F_{th}(t)$ is obtained with the tabulated values of $|Q|$ and $|\Phi|$. However, the theoretical curve is still underdamped in comparison with the experimental, which suggests the participation of triple collisions in the absorption process. The long time tail of $F_{th}(t)$ would be modified by accounting for $\Delta J_1 = \Delta J_2 = 0$ absorptions, which Ho *et al.*[5] expect to be important at $< 10\ cm^{-1}$ approximately.

CYANOGEN

In this case of limiting molecular anisotropy, reasonable normalised lineshape agreement, represented by $F_{th}(t)$ and $F_{exp}(t)$, cannot be obtained (fig. 3). The values of $|Q|$ and $|\Phi|$ tabulated are those for curve 2 of fig. 3. The only satisfactory feature is that these values of $|Q|$ and $|\Phi|$ confirm an intuitive expectation of certainly a large molecular quadrupole moment, and possibly a large hexadecapole moment as well. The $F_{th}(t)$ curves are not underdamped compared with $F_{exp}(t)$, which suggests that triple collisions are not important at 33.5 bar. Attempts to modify the present theory with angle dependent intermolecular potentials such as $U_{AA}(R)+U_{QQ}$ will have no effect on the normalised lineshape because [5] U_{QQ} is independent of the rotational state of a molecule provided the rotational wavefunctions are assumed to be unperturbed. Use of $U_{AA}(R)+U_{QQ}$ might mean a small change in the relative values of A_n, but this is unlikely (fig. 3) to produce lineshape agreement. The absolute values of $|Q|$ and $|\Phi|$ will, of course, be altered significantly.

The importance of choosing reasonable values of the Lennard-Jones parameters ε/k and σ has been pointed out.[15, 16] While the absolute values of $|Q|$ and $|\Phi|$ are certainly very sensitive [9, 17] to the choice of these variables, the relative values of A_n will not be changed much since the ratio of the Buckingham/Pople functions [13] $H_8(y(\varepsilon/kT))/H_{12}(y(\varepsilon/kT))$ is very slowly varying with ε/k. Therefore ε/k and σ have little effect on the normalised lineshape represented by $F_{th}(t)$. A theory of pressure induced absorption is needed which either disposes with point multipole expansions of the molecular electrostatic field [18] at a point R, or retains this approximation and then proceeds (albeit rather discordantly) to take into account the effect of molecular anisotropy on the eigenstate of a pair of molecules.

Following the treatment of Gordon,[10] it can be shown that:

$$\int_{-\infty}^{\infty} I_{th}(\bar{\nu}) \exp(i\omega t)\, d\omega$$
$$\propto \int_0^{\infty} \langle \mu^{AA}(0, R) \cdot \mu^{AA}(t, R)\rangle \cdot 4\pi R^2 \exp(-U_{AA}(R)/kT)\, dR$$

which represents a radial average of a time and R dependent dipole correlation function $\langle \boldsymbol{\mu}^{AA}(O,R) \,.\, \boldsymbol{\mu}^{AA}(t,R)\rangle$. This gives a little insight to the physical significance of $I_{th}(\bar{\nu})$ and thus of $F_{th}(t)$.

U.C.W. Aberystwyth, and the S.R.C. (through a post-doctoral fellowship) are thanked for financial support.

[1] M. Evans, *J.C.S. Faraday II*, 1975, **71**, 71.
[2] J. P. Colpa and J. A. A. Ketelaar, *Mol. Phys.*, 1958, **1**, 343.
[3] B. S. Frost, *J.C.S. Faraday II*, 1973, **69**, 1142.
[4] D. R. Bosomworth and H. P. Gush, *Canad. J. Phys.*, 1965, **43**, 751.

[5] W. Ho, G. Birnbaum and A. Rosenberg, *J. Chem. Phys.*, 1971, **55**, 1028.
[6] M. Evans, *J.C.S. Faraday II*, 1973, **69**, 763.
[7] M. Evans, *Mol. Phys.*, 1975, in press.
[8] A. I. Baise, *J. Chem. Phys.*, 1974, **60**, 2936.
[9] G. J. Davies and M. Evans, *J.C.S. Faraday II*, in press.
[10] R. G. Gordon, *J. Chem. Phys.*, 1965, **43**, 1307.
[11] R. C. Singleton, *Comm. Assoc. Comput. Mach.*, 1968, **11**, 773.
[12] R. C. Singleton, *Comm. Assoc. Comput. Mach.*, 1969, **12**, 187.
[13] A. D. Buckingham and J. A. Pople, *Trans. Faraday Soc.*, 1955, **51**, 1173.
[14] H. A. Stuart, *Molekülstruktur* (Springer, Berlin, 1967), chap. 8, p. 416.
[15] T. G. Copeland and R. H. Cole, *Chem. Phys. Letters*, 1973, **21**, 289.
[16] R. H. Cole, personal communication.
[17] J. E. Harries, *J. Phys. B*, 1970, **3**, 704; 1970, **3**, L150.
[18] G. J. Davies, J. Chamberlain and M. Davies, *J.C.S. Faraday II*, 1973, **69**, 1223.

PRINTED IN GREAT BRITAIN AT
THE UNIVERSITY PRESS
ABERDEEN